





## RADIOCARBON STEP-COMBUSTION OXIDATION METHOD AND FTIR ANALYSIS OF TRONDHEIM CaCO<sub>3</sub> PRECIPITATES OF ATMOSPHERIC CO<sub>2</sub> SAMPLES: FURTHER INVESTIGATIONS AND INSIGHTS

Guaciara M Santos<sup>1\*</sup>  • Christopher A Leong<sup>1</sup> • Pieter M Grootes<sup>2</sup>  • Martin Seiler<sup>2</sup>  • Helene Svarva<sup>2</sup>  • Marie-Josée Nadeau<sup>2</sup>

<sup>1</sup>Earth System Science, University of California, Irvine, B321 Croul Hall, Irvine, CA 92697-3100, USA

<sup>2</sup>The National Laboratory for Age Determination, NTNU University Museum, 7033 Trondheim, Norway

**ABSTRACT.** Eight atmospheric carbon dioxide samples (as calcium carbonate—CaCO<sub>3</sub>—precipitates) from Lindesnes site (58°N, 7°E), belonging to 1963 and 1980 (four samples from each year) and stored at the National Laboratory for Age Determination (NTNU), have been reevaluated through radiocarbon (<sup>14</sup>C) analysis. Previous <sup>14</sup>C results indicated the presence of a contaminant, which was not removed through different chemical cleansing procedures (e.g., hydrochloric acid—HCl and/or hydrogen peroxide—H<sub>2</sub>O<sub>2</sub>). Here, we present a follow up investigation using <sup>14</sup>C step-combustion and Fourier-transform infrared spectroscopy (FTIR) analysis. Results from <sup>14</sup>C data indicate unsuccessful removal of the contaminant, while further FTIR analysis displayed the presence of moisture. This finding alludes to the possibility that the contaminant is of ambient air-CO<sub>2</sub> deeply embedded in CaCO<sub>3</sub> powders (within clogged CaCO<sub>3</sub> pores and/or bonded to the lattice). Samples were found exposed to air-CO<sub>2</sub> and humidity. These conditions may have lasted for years, possibly even decades, leading to the <sup>14</sup>C offsets detected here.

**KEYWORDS:** atmospheric <sup>14</sup>C reconstructions, CaCO<sub>3</sub> storage, CO<sub>2</sub> precipitated carbonate.

### 1. INTRODUCTION

An archive of atmospheric CO<sub>2</sub> (as calcium carbonate—CaCO<sub>3</sub>—precipitates) from Lindesnes site (58°N, 7°E), stored at the National Laboratory for Age Determination (NTNU), formerly Trondheim Radiocarbon Laboratory has been evaluated through radiocarbon (<sup>14</sup>C) analysis for its reliability (Seiler et al. 2023). Carbonate precipitates were sampled as described in Nydal and Lövseth (1983). The CaCO<sub>3</sub> powders have been stored since the 1960s in distinct glass vials with closures (Figure 1). The 1980s jars and lids (type B1 and B2) seem to offer better seal (Seiler et al. 2023). Still, containers were found in a room without climate controls. A thorough <sup>14</sup>C investigation conducted by Seiler et al. (2023), commenced by using different chemical cleansing procedures (e.g., hydrochloric acid—HCl and/or hydrogen peroxide—H<sub>2</sub>O<sub>2</sub>), indicated the presence of a contaminant. Regardless of multiple chemical attempts for contamination removal and different methods to evolve its carbon content, offsets from expected atmospheric <sup>14</sup>C values were as high as 160‰. This finding suggested that the pollutant was somewhat embedded in the carbonate precipitates.

There is a vast array of atmospheric CO<sub>2</sub> samples in CaCO<sub>3</sub> powder stored at NTNU that has not been measured yet (> 1000 samples; see Seiler et al. 2023 for details). Even though efforts to reproduce Nydal's historical <sup>14</sup>C results (Nydal and Lövseth 1983) after CaCO<sub>3</sub> powder chemical cleansing were disappointing (Seiler et al. 2023), further investigations were performed here to gain insight on possible contamination sources, and maybe secure its removal. Assuming that the contaminant was somewhat sensitive to heat treatments at lower temperatures (e.g., lower than 375°C, a temperature setting that is high enough to remove labile organic carbon, but sufficiently low to avoid charring, Currie et al. [2002] or Szidat et al. [2013]), additional analyses

\*Corresponding author. Email: [gdossant@uci.edu](mailto:gdossant@uci.edu)



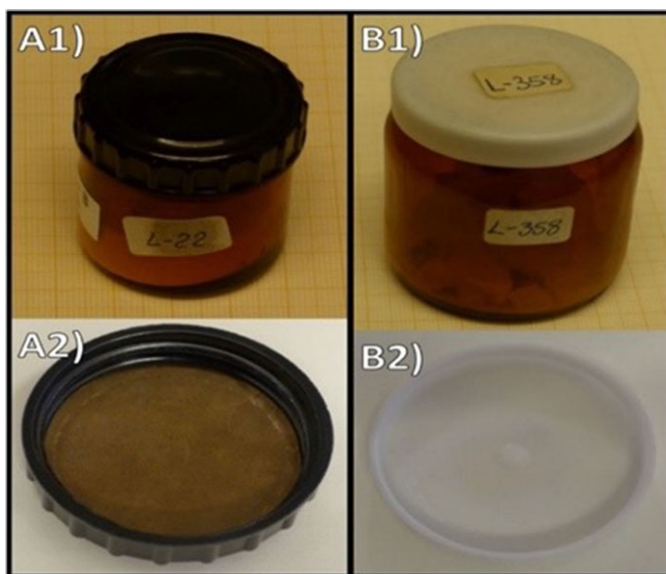


Figure 1 Types of containers and lids from the subset of stored  $\text{CaCO}_3$  powder samples reevaluated in this study and adapted from Seiler et al. (2023). Early 1960s samples were stored in type 1 container (panels A1 and A2), while 1980s used type 2 container (panels B1 and B2). Nydal and Lövseth (1983) used a 0.5 N sodium hydroxide (NaOH) solution in an open dish to absorb atmospheric  $\text{CO}_2$  over a 4-to-7-day period. While the Nydal and Lövseth (1983) article does not explicitly describe how the  $\text{CaCO}_3$  was precipitated afterwards, a previous work by Nydal (e.g., Nydal 1966) describes the usage of  $\text{CaCl}_2$  [ $\text{CaCl}_2$  reacts with  $\text{Na}_2\text{CO}_3$  to produce  $\text{NaCl}$  and a  $\text{CaCO}_3$  precipitate].

were carried out. These included (i) a  $^{14}\text{C}$  two-step thermal oxidation to remove adsorbed/absorbed  $\text{CO}_2$  and/or labile organic carbon (OC) from  $\text{CaCO}_3$  precipitate powders, and (ii) Fourier-transform infrared spectroscopy (FTIR) analysis of the step-combustion treated and untreated  $\text{CaCO}_3$  powders. While our new efforts did not produce Nydal's historical  $^{14}\text{C}$  results, offsets were still similar to those obtained by Seiler et al. (2023), we provided new insights on the carbon contaminant of Nydal's  $\text{CaCO}_3$  precipitate archive.

## 2. SAMPLES AND METHODS

### 2.1. Sample Selection

Besides the subset of the  $\text{CaCO}_3$  samples from NTNU's archive (addressed below), we also selected reference materials of carbonate and organic sources to be subjected to the same sample processing steps as carbonate precipitates. Samples are briefly described below.

1. Nydal's 1963 and 1980 set— $\text{CaCO}_3$  precipitates of atmospheric  $\text{CO}_2$  samples sampled by Nydal and Lövseth (1983) and stored in types 1 and 2 containers, respectively (Figure 1, reproduced from Seiler et al. 2023).
2. Calcite—Clear calcite crystal used at the Keck Carbon Cycle Accelerator Mass Spectrometer facility of the University of California, Irvine (KCCAMS/UCI) as an in-house blank for several years ( $\text{F}^{14}\text{C} = 0$  or  $^{14}\text{C}$ -free), e.g., Santos et al. (2007), Hinger et al. (2010), Bush et al. (2013).

3. Coral standard—This relatively modern coral sample ( $F^{14}\text{C}$  is  $0.9440 \pm 0.0004$ ; Hinger et al. 2010) is another in-house reference material that has been repeatedly used in several projects (Bush et al. 2013, Gao et al. 2014).
4. FIRI-C—Marine turbidite samples from the Fourth International Radiocarbon Intercomparison (FIRI). The consensus  $^{14}\text{C}$  age of FIRI-C has been reported as  $18,176 \pm 10.5$  yrs BP (Scott et al. 2004), when  $\text{CO}_2$  evolved has been produced by acid hydrolysis. This material is a carbonate/clay mixture with  $< 50\%$  carbonate, several minerals and a younger organic carbon fraction (Bush et al. 2013). It was chosen for this experiment due to this characteristic.
5. USGS coal—Argonne Premium Coal POC#3, collected during the United States Geological survey (Vorres 1990), was used as an independent reference blank material ( $F^{14}\text{C} = 0$  or  $^{14}\text{C}$ -free). This highly recalcitrant organic sample was added to this study to evaluate the background processing of treatments, during removal of surface carbon by heat.
6. Rice Char—Rice charcoal from University of Zurich containing both organic and elemental/recalcitrant carbon. It was used in our experiment to evaluate the effectiveness of the removal of OC during heat treatment. Consensus of its recalcitrant fraction (also termed EC—elemental-carbon fraction), after organic carbon removal, is  $F^{14}\text{C} = 1.0675 \pm 0.0007$  ( $n=3$ ) (Huang et al. 2021).

## 2.2. Sample Preparation and Handling

### 2.2.1. Radiocarbon Sample Processing and Measurements

For carbonate samples ( $\text{CaCO}_3$  precipitates, calcite and coral standard), various amounts between 8.0 and 12 mg of chemically untreated material were loaded into prebaked quartz tubes of about 15 cm long with 40 to 50 mg of copper oxide ( $\text{CuO}$ ), used as a catalyst to oxidize the samples (Table S1). Loaded tubes with samples were placed upright on an in-house modified reaction heat block from Corning PC-400D set to a maximum of  $285^\circ\text{C}$  for 24 hr. This temperature setting was thoroughly tested for its stability. Moreover, this temperature is higher than that reported by Santos et al. (2010) when removing adsorbed/absorbed  $\text{CO}_2$  and carbon embedded in porous powders (i.e.,  $160^\circ\text{C}$ ), and slightly lower than the typical temperatures reported to evolve OC without charring, when heating is conducted under air or pure oxygen (i.e.,  $340^\circ\text{--}375^\circ\text{C}$  during  $< 1$  to 24 hr; Szidat et al. 2013). Thus,  $285^\circ\text{C}$  for 24 hr was chosen for our first-step combustion oxidation method.

About 5–6 cm of the lower end of each quartz tube with loaded materials was inserted into the heating element holes, while the remaining portions of the tube received heat transferred from below. To avoid contaminants falling into quartz tube openings during the course of the treatment, and while OC was being removed, a large heavy-duty aluminum foil tent was set up over the heat block set. Precise maximum heating of the heat block set was checked during, and after treatment by an independent temperature probe (Precision RTD Handheld Data Logger Thermometer). Upon 24 hr, quartz tubes with loaded samples were transferred still hot to the vacuum line (to avoid reabsorption of  $\text{CO}_2$  from air), evacuated and sealed off with a flame torch for combustion. Samples were then heated to  $1000^\circ\text{C}$  per 6 hr (or  $900^\circ\text{C}$  over 3 hr) to extract  $\text{CO}_2$  (details in Tables S1 and S2). Quartz tubes were carefully laid down horizontally after powders and  $\text{CuO}$  were well distributed within, as some etching from inside out was expected (Santos and Xu 2017). Several of the tubes combusted at  $1000^\circ\text{C}$  per 6 hr ruptured during the procedure, especially those loaded with calcite, coral standard or FIRI-C. For

CaCO<sub>3</sub> precipitates, higher CO<sub>2</sub> yields were obtained from those with > 10 mg, combusted at 1000°C over 6 hr, although some variability was detected (Table S1). The organic reference standards (USGS coal and Rice char), which were selected for comparisons, were handled under the same methods. Their weights were adjusted according to their EC content, e.g., 1 mg for USGS coal (80–100% EC) and about 6.5 mg for Rice Char (15–30% EC). Sealed tube combustion evolved CO<sub>2</sub> were cryogenically cleaned using a vacuum line, and later transferred to a graphitization vessel to produce filamentous graphite following specific protocols (Santos and Xu 2017).

Radiocarbon measurements were taken on a modified compact AMS system with <sup>13</sup>C/<sup>12</sup>C measurement capabilities (NEC 0.5MV1.5SDH-1) (Beverly et al. 2010). For normalization and quality assessment of spectrometer, 6 oxalic acid I (OX-I) targets, an oxalic acid II (OX-II) from NIST and a sucrose from ANU were also measured with samples. Sample preparation backgrounds have been subtracted, based on measurements of <sup>14</sup>C-free calcite and USGS coal. Radiocarbon concentrations are given as fractions of the Modern standard and/or conventional radiocarbon age (Tables S1 and S2), following the conventions of Stuiver and Polach (1977) and Reimer et al (2004). All <sup>14</sup>C results have been corrected for isotopic fractionation, based on spectrometer AMS online-δ<sup>13</sup>C values derived from <sup>12</sup>C and <sup>13</sup>C loop-by-loop measured from the same graphite targets (Beverly et al. 2010).

### 2.2.2. Fourier Transform Infrared Spectroscopy (FTIR) Analysis

As for FTIR measurements, just CaCO<sub>3</sub> precipitates and FIRI-C were analyzed. Samples were processed as followed—one set was kept untreated, while another was heated to a maximum of 285°C for 24 hr in air (as described above—section 2.2.1) in shell glass vials. Sample weights (in mg) before and after heating were carefully recorded. Mass percentage variation was higher among the CaCO<sub>3</sub> precipitates (0 to 15%), while FIRI-C showed a difference of 9%.

Vials of untreated and step-combustion treated samples were kept closed by a tight insert cap until measurements were performed at the Laser Spectroscopy Labs at the University of California, Irvine. Heat treated samples were measured within less than 24 hr of treatment, in order to preserve freshness. Analyses were performed using a JASCO FT/IR-4700 spectrometer with measuring transmittance values set between the spectral range of 4000 to 400 cm<sup>-1</sup> and with data intervals at 0.482117 cm<sup>-1</sup>, as standard conditions for all measurements. For clarity, the wavenumber window shown here starts at 600 cm<sup>-1</sup> to avoid the noise area at the low wavenumber end of each spectrum.

## 3. RESULTS AND DISCUSSIONS

### 3.1. Radiocarbon Results

The complete set of CaCO<sub>3</sub> precipitate <sup>14</sup>C results as well as those of reference materials are reported in Tables S1 and S2 (supplementary material). Target sizes (in mg C) vary significantly, e.g., 0.22 to 0.97 mg C. Notably, minimum CO<sub>2</sub> yields were obtained for pure calcite and coral standard, where particles loaded in quartz tubes were significantly coarser than the fine powders of Nydal's CaCO<sub>3</sub> precipitates.

Literature searches show that carbonate decomposition should occur at temperatures as low as 850°C (Stern 1969). Even so, absolute pressure in the calciner environment (Maya et al. 2018), size of the CaO crystallites formed under heat, mineral and organic impurities (Galwey and Brown, 1999) can also play a role in CaO reactivity and CO<sub>2</sub> release. Here, carbonate samples were loaded in an evacuated quartz tube with no partial pressure, until CuO was finally

activated. Reactivity of CaO and its sintering against inner quartz tubes walls may have diminished the access to carbon during the CaCO<sub>3</sub> decomposition reaction. Plus, we cannot rule out CO<sub>2</sub> recombination with the CaO leftover and/or CuO, once quartz tubes returned to room temperature after combustion. We also used two temperature settings for sealed quartz tubes combustion and time durations (1000°C per 6 hr and/or 900°C over 3 hr), and distinct sample weights (8–12 mg; see Tables S1 and S2). All of the above, may have affected the CaCO<sub>3</sub> decomposition response during sealed tube combustion step.

Nonetheless, lower graphite mass (as mg C) and its impact on <sup>14</sup>C results were addressed by background mass balance correction, using blanks treated in the same fashion as the other samples. For that, we used 7 blanks (2 calcites and 5 USGS coals) of different masses (Table S2). Their <sup>14</sup>C concentration (relative to modern standard) and masses (as mg C) were plotted to derive the constant mass of contamination introduced during the entire sample processing (step-combustion, seal-off combustion, graphitization, and pressing) plus measurement at the spectrometer (Figure S1). A consistent value of 1 µg C modern blank was found, as <sup>14</sup>C results of calcites and coals overlapped. Thus, this constant blank mass was used for <sup>14</sup>C results background correction, following the equations in Santos et al. (2007).

As mentioned earlier, we also determined AMS online-δ<sup>13</sup>C values derived from <sup>12</sup>C and <sup>13</sup>C loop-by-loop measured from the same graphite targets (not shown here). The AMS online-δ<sup>13</sup>C values based on Nydal's CaCO<sub>3</sub> precipitates were significantly lighter (e.g., δ<sup>13</sup>C = -20‰ in average) than what one would expect for a CaCO<sub>3</sub> matrix. The NaOH-static method, the one used by Nydal to capture atmospheric CO<sub>2</sub> during several days, tend to introduce large isotope fractionation in <sup>13</sup>C (e.g., -15 to -25‰, according to Turnbull et al. [2017]) due to the high alkalinity of NaOH. In Nydal and Lövseth (1983), the CaCO<sub>3</sub> precipitates δ<sup>13</sup>C values reported ranged from -25 to -27‰ and were used for the intended purpose of correcting <sup>14</sup>C data. When δ<sup>13</sup>C was not measured, its value was then estimated based on multiple samples (see details in Nydal and Lövseth 1996). Since at KCCAMS/UCI, isotopic fractionation correction to <sup>14</sup>C data is performed by using the AMS online-δ<sup>13</sup>C values, the effect of chemical reaction shifts, machine and size dependence (if any) were completely addressed and removed. For more details on data analysis, see Santos et al. (2007, 2010).

Overall, duplicated <sup>14</sup>C results as well as those of reference materials support the reliability of the measurements. The carbonate samples, L26 and FIRI-C, overlap in ±2σ of each other (Table S1). Paired <sup>14</sup>C results of the samples L22B, L24, and L28 showed larger differences, e.g., more than ±2σ. Note that carbonate samples did not undergo chemical leaching by a weak HCl treatment (Santos et al. 2004) before step-combustion, and this may have played a role. Lower temperature step-combustion is expected to remove just OCs, and not secondary carbonates. Another possibility is that the CaCO<sub>3</sub> precipitates contamination is not homogeneous, and distinct initial combusted masses resulted in uneven <sup>14</sup>C signatures (see further discussion in 3.4 section). Replicated <sup>14</sup>C results of the recalcitrant fraction of the Rice char overlap with each other as well as accurately reproduce its expected consensus <sup>14</sup>C value (Table S2). Paired FIRI-C turbidite <sup>14</sup>C results also overlapped with each other.

In figure 2 we compared UCI <sup>14</sup>C results of CaCO<sub>3</sub> precipitates as F<sup>14</sup>C with those reported by Nydal and Lövseth (1983) and those recently measured at NTNU by Seiler et al. (2023). In the latter, we chose the set of <sup>14</sup>C results from CaCO<sub>3</sub> powders subjected to just flash-combustion using an elemental analyzer for comparisons. Both NTNU and Nydal's values were also reproduced in Table S1 to serve as reference. For a complete overview of chemical treatments

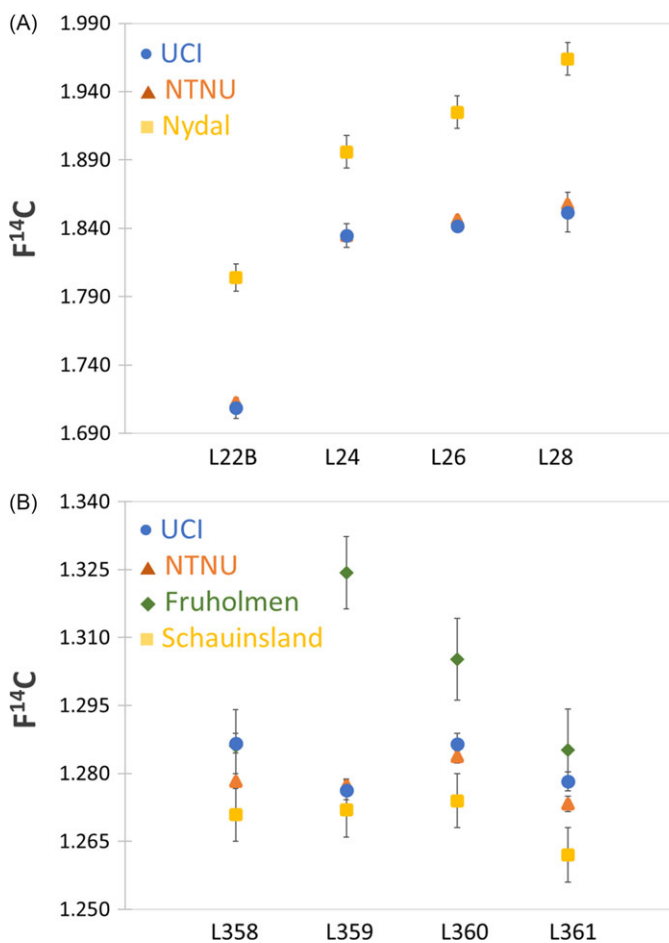


Figure 2 Radiocarbon results as  $F^{14}C$  values for both the 1963 (panel A) and 1980 (panel B) series from different works are shown. Note that panels show very distinctive y-axis scales. Color labels inserted in distinct plot areas discriminate the results from UCI (this study), NTNU (Seiler et al. 2023), Nydal (Nydal and Lövseth 1983), Fruholmen (Nydal and Lövseth 1996) and/or Schauinsland (Levin et al. 1985).

attempts to remove contaminants from the  $CaCO_3$  powders stored at NTNU, please refer to Seiler et al. (2023).

For simplicity's sake, in Figure 2 we averaged the UCI  $^{14}C$  results of  $CaCO_3$  precipitates produced in duplication and used the greater error of the two, individual error or standard deviation of the paired  $^{14}C$  results, as error bar. According to Nydal's runlog books, the 1963 samples measured here, and by Seiler et al. (2023), were indeed measured by  $^{14}C$  before moving to storage in vial type 1 (Figure 1). Regarding the  $CaCO_3$  precipitate 1980 series, they were not measured by Nydal in the past. Following Seiler et al. (2023) approach, atmospheric  $^{14}C$  values of Schauinsland (48°N) (Levin et al. 1985) are loosely used here, as reference for the  $^{14}C$  results of the  $CaCO_3$  precipitate 1980 series. We also added data from Fruholmen (71°N) (Nydal and Lovseth 1996) during the same period, as a way to bracket the  $^{14}C$  results of Lindesnes (58°N) site.

For the most part, current  $\text{CaCO}_3$  precipitate  $^{14}\text{C}$  results obtained at UCI (this study) and at NTNU (Seiler et al. 2023) are in agreement with each other, especially those belonging to the 1963 series (Figure 2A). For the  $\text{CaCO}_3$  precipitates 1980 series (Figure 2B), L358  $^{14}\text{C}$  results between UCI and NTNU are visibly apart from each other (standard deviation = 0.6%). For detailed differences in  $^{14}\text{C}$  data and assemblages, see Table S1. Radiocarbon data agreements between UCI and at NTNU sets are remarkably good for samples that undergo different handling procedures, spectrometer measurement setups, and data analyses, especially when the contamination embedded into  $\text{CaCO}_3$  powders was clearly not removed. As Seiler et al. (2023) already pointed out, the  $^{14}\text{C}$  results of  $\text{CaCO}_3$  powders from the 1980 series are higher than those from the Schauinsland (48°N) site reported by Levin et al. (1985) (Figure 2B). The Schauinsland (48°N) site is located 10° further south than Lindesnes (58°N), and therefore, the geographical provenance of the air parcels transporting  $^{14}\text{CO}_2$  reaching those sites may explain the differences observed here. As aforesaid, we also plotted the dataset of Fruholmen (Nydal and Lövseth 1996) for comparisons (Figure 2B). This geographic location is approximately 10° north of the Lindesnes (58° N) site. The fact that our  $^{14}\text{C}$  results fell between  $^{14}\text{CO}_2$  signatures of both Schauinsland (48°N) and Fruholmen (71°N) could be somewhat promising. Yet, the results of a series of archaeological samples, archived in the same type 2 containers (Figure 1), indicate potential atmospheric contamination (Seiler et al. 2023). Without further atmospheric  $^{14}\text{C}$  results in very close proximity to the Lindesnes (58°N) site, it cannot be substantiated whether the  $^{14}\text{C}$  results of the  $\text{CaCO}_3$  precipitates of the 1980 series of either Seiler et al. (2023) or this study are correct.

As per the reference materials (Table S2), sealed tube combusted step-combustion carbonates FIRI-C turbidite yielded a  $^{14}\text{C}$  age of  $18,380 \pm 57$  (n=2) yrs BP, while coral standard a  $F^{14}\text{C}$  of  $0.9435 \pm 0.0015$  (Table S2). Both are in reasonable agreement with expected consensus values (reported in section 2.1), especially coral standard. FIRI-C showed a small  $^{14}\text{C}$ -age difference of about 200 yrs between sealed tube step-combustion at 285°C (this study) and its consensus value, which is based on the standard acid hydrolyze procedure (Scott et al. 2004). This difference is significantly smaller than that reported by Bush et al. (2013), e.g., 2–4 kyrs offsets, when mixed carbon fractions of this turbidite were directly measured by  $^{14}\text{C}$ -AMS when loaded into aluminum target holders. Bush et al. (2013) also attempted to remove the  $^{14}\text{C}$  effect of the FIRI-C organic fraction by heating this turbidite at 500°C in air. While the authors failed to reproduce expected  $^{14}\text{C}$  results of Scott et al. (2004), they demonstrated that the FIRI-C turbidite powder is highly active, and can reabsorb  $\text{CO}_2$  from ambient, once powders are allowed to cool off. Santos et al. (2010) demonstrated a similar effect when heating fine powders at 160°C. Thus, this issue seems to be related to absorption properties of materials in particulate form, their porosity level, and particulate surface area available, rather than just temperature settings for the purpose of cleansing.

Here, all samples (in the form of coarse particulates or powders, carbonates or organics) were not allowed to cool off after 285°C treatment per 24 hr. Thus, we have no knowledge if reabsorption effects would be different between distinct types of particulate samples. While our FIRI-C two step-combustion oxidation age-value of  $18,380 \pm 57$  (n=2) yrs BP is somewhat older than that reported in Scott et al. (2004), it is not significantly different. Radiocarbon result of the recalcitrant fraction of organic Rice char yielded  $F^{14}\text{C}$  of  $1.0655 \pm 0.0020$  (n=4), and is in perfect alignment with its expected  $^{14}\text{C}$  value (section 2.1). We can then conclude that nearly all OC have been removed from both FIRI-C and Rice char upon step-combustion treatment, as described in section 2.2.1.

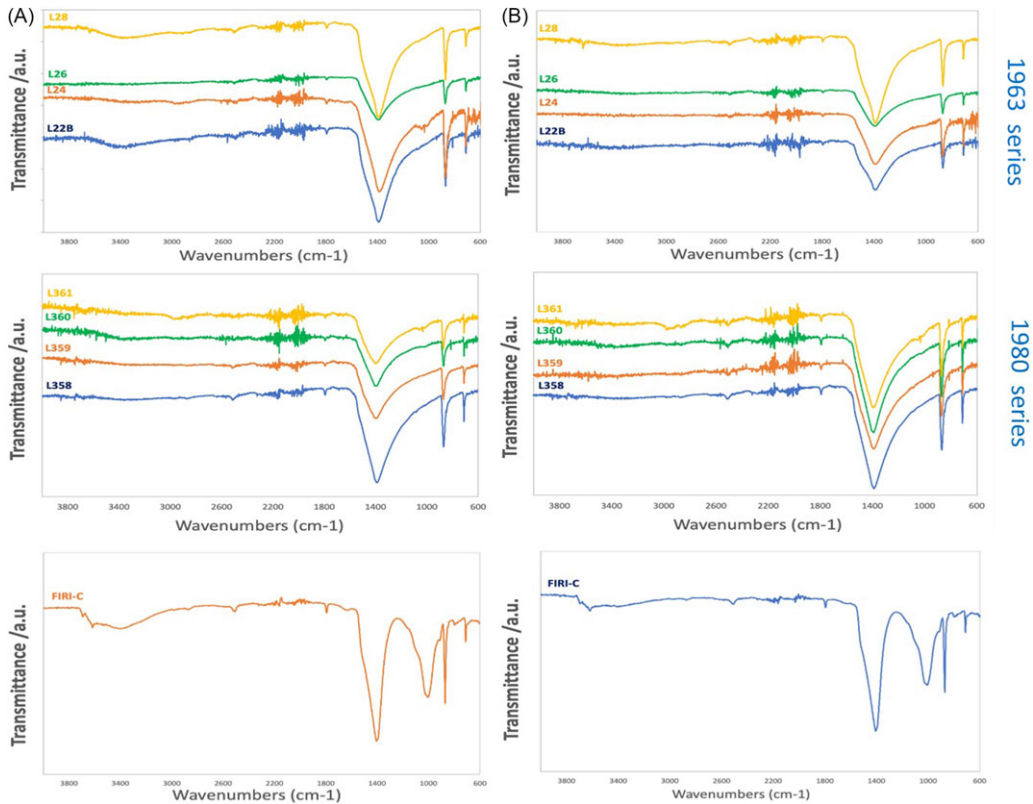


Figure 3 FTIR spectrum of untreated (panel A) and heat-treated (panel B) CaCO<sub>3</sub> powders from 1963 and 1980, as well as FIRI-C turbidite (carbonate/clay mixture). The window was set between 4000 to 600 cm<sup>-1</sup>.

### 3.2. FTIR Results

FTIR spectroscopy was performed to help determine possible CaCO<sub>3</sub> precipitate impurities (Figure 3). FIRI-C, a carbonate/clay mixture, was also analyzed in view of its heterogeneous properties. Typical FTIR of simple molecules, such as calcium carbonate (CaCO<sub>3</sub>), water (H<sub>2</sub>O), sodium hydroxide (NaOH) and sodium chloride (NaCl) are shown in the supplementary material (Figure S2) to assist in discussions.

All FTIR CaCO<sub>3</sub> precipitate profiles of untreated (Figure 3A) and step-combustion treated (Figure 3B) samples show the presence of the usual CaCO<sub>3</sub> profile peaks between 1500 and 700 cm<sup>-1</sup> (Figure S1), e.g., the pronounced and broad peaks (1400, 865, and 714 cm<sup>-1</sup>). Those are characteristic peaks of CaCO<sub>3</sub> molecules and calcite crystals (Gupta et al. 2015; NIST webbook online database—Figure S2). The FIRI-C untreated and heated-treated samples showed the IR band at 1022 cm<sup>-1</sup> due to Si-O-Si stretching vibration characteristic of sediments (Liu et al. 2013).

FTIR spectrum indicate that three of the 1963 untreated CaCO<sub>3</sub> powders were still slightly wet, possibly due to CaCO<sub>3</sub> powders exposed to moist air during storage. While no post-treatment procedures are detailed in Nydal and Lövsæth (1983), we assume that carbonate precipitate washing was sufficient to remove Na residues from incomplete removal



of supernatant (NaOH) and reaction byproducts (NaCl). Nonetheless, we added here the transmittance peak profiles of pure H<sub>2</sub>O as well as NaOH and NaCl (Figure S2). Their transmittance peaks most likely overlap in the same fingerprint broad region (2500–3750 cm<sup>-1</sup>), and therefore, they would be difficult to disentangle in any FTIR profile, especially if they are subtle.

The 1980 series had little to no peaks within the 2500–3750 cm<sup>-1</sup> region before and after heat-treatment (Figure 3B), indicating that these samples were somewhat drier, than those of the 1963 series (Figure 3A). The rationality behind peak differences between 1963 and 1980 series samples may be explained by types of containers and lids (Figure 1). As Seiler et al. (2023) noted, cap type 2 seems to provide better closure than cap type 1.

The FIRI-C untreated and heated-treated samples also showed FTIR profile differences by the reduction of the broad area of the single bond between 2500–4000 cm<sup>-1</sup>. This area is known to contain aromatic C-H and C-C bonds, as well as overlapping νH-O (H<sub>2</sub>O). A reduction of this broad band, but not its complete removal, would imply that some of the recalcitrant C-H and C-C bonds are still present after heat treatment. Unremoved recalcitrant fraction of FIRI-C may corroborate the small <sup>14</sup>C-age difference of about 200 years from sealed tube step-combustion (this study). Even though in our procedure samples were transferred hot to vacuum line for evacuation and sealing (so that ambient-air CO<sub>2</sub> reabsorption over fine powders could be avoided), any unremoved elemental/refractory carbon would be combusted in conjunction with CaCO<sub>3</sub> in the presence of CuO. The evolved CO<sub>2</sub> (and its associate <sup>14</sup>C value) would therefore be biased by this sediment-like carbon contribution.

### 3.3. Nydal's Stored CaCO<sub>3</sub> Precipitates and Possible Sources Exogenous C Contamination

Nydal's CaCO<sub>3</sub> precipitates have been stored in a room at NTNU without climatic condition controls (variable temperature and relative humidity). While containers with CaCO<sub>3</sub> precipitates (retested in this study) appeared to be properly closed at first glance, there is no guarantee that this was the case for the whole storage period. Moreover, the lid from the type 1 container appears to be less air-sealing effective than that of type 2 (Figure 1). The possibility of decades of exposure to moisture, increased air-CO<sub>2</sub> and variable temperatures, leads us to consider some theories on how CaCO<sub>3</sub> precipitates have been contaminated.

First, ambient CO<sub>2</sub> that seeped into containers could be adsorbed as such in CaCO<sub>3</sub> precipitate inter- and intra-particle voids. While we have not conducted porosimetry analysis of Nydal's CaCO<sub>3</sub> precipitate, it is fair to assume that the powder is highly porous, as judged by bio- and industrially produced CaCO<sub>3</sub> precipitates that have been heavily studied for their permeability characteristics and CO<sub>2</sub> storage capabilities (e.g., Moore and Wade 2013; Yoon et al. 2017). Moreover, the large specific surface area of all types of finer powders and the interstitial gaps created by particles of different sizes tend to naturally entrap gasses. Nonetheless, adsorbed ambient CO<sub>2</sub> within and between particles is normally very volatile and sensitive to heat treatments as low as 160°C (Santos et al. 2010). If the main contaminants of Nydal's stored CaCO<sub>3</sub> precipitates are interparticle OCs and/or other gasses, they should have been mostly removed upon step-combustion treatment, as we demonstrated by <sup>14</sup>C measurements of step-combustion Rice char and FIRI-C samples (Table S2). Moreover, partial OC removal of Nydal's stored CaCO<sub>3</sub> precipitates by step-combustion would at least lead to measurable differences between <sup>14</sup>C step-combustion treated CaCO<sub>3</sub> results and those of Seiler et al. (2023). We have not observed these differences, thus solo ambient air-CO<sub>2</sub>

contamination does not seem to explain the mismatch between current and Nydal's  $^{14}\text{C}$  results.

A second hypothesis involves re-carbonation of ambient- $\text{CO}_2$  and formation of new layers of carbonate over and within intraparticle voids of the existing  $\text{CaCO}_3$  powders, a type of  $\text{CO}_2$ -water-rock interaction at room-temperature (small amounts of hydrate lime— $\text{Ca}(\text{OH})_2$ , for example). For a significant secondary formation of  $\text{CO}_2$  to  $\text{CaCO}_3$  microspheres into more stable  $\text{CaCO}_3$  crystalline forms at room temperature, pre-calcination of  $\text{CaCO}_3$  to  $\text{CaO}$  at higher temperatures is required (Erans et al. 2020). While we do not believe Nydal's  $\text{CaCO}_3$  precipitates undergo calcination, there is very little information on how they were handled. Among the numerous factors that can affect the  $\text{CaCO}_3$  precipitation process and secondary species formation, Febrida et al. (2021) stress the presence of various foreign ions or molecules depending on the aqueous solution used from which the carbonate precipitates. For sample collection, Nydal used rainwater (Nydal and Lövseth 1983), which can be loaded with several ionic compounds (Carol 1962). Therefore, the combination of high air- $\text{CO}_2$  pressures found in buildings (as far as 2500 ppm—Erans et al. 2020),  $\text{CO}_2$  solubility property in liquid water or vapor (Zeman and Lackner 2004), and the fact that the Nydal's  $\text{CaCO}_3$  powder containers were found in a room with moisture variability for 30+ years of storage may have played a role in further air- $\text{CO}_2$  entrapment, soluble calcium bicarbonate formation ( $\text{H}_2\text{CO}_3$ ), and  $\text{CaCO}_3$  recrystallization filling up  $\text{CaCO}_3$  pores, especially if foreign ions were present in precipitates (Sanz-Pérez et al. 2016; Giacomini et al. 2020; Toffolo 2020; Febrida et al. 2021). Thus, ambient  $\text{CO}_2$  adsorbed to  $\text{CaCO}_3$  powders may just have promoted a dynamic and continuous gas-solid exchange process with  $\text{CO}_2$  bonding to the lattice. Dissolved  $\text{CO}_2$  reacts with crystals through a  $\text{CO}_2$ -water-rock interaction, where  $\text{H}_2\text{CO}_3$  and  $\text{HCO}_3^-$  secondary species are formed (Yoon et al. 2017; Hanein et al. 2021; Huang et al. 2021). Once in the interior of minute particles, this exchanged  $\text{CO}_2$  may no longer be easily removed by either heating at lower temperatures (this study) or selective leaching (Seiler et al. 2023). The latter may explain why the  $^{14}\text{C}$  results of  $\text{CaCO}_3$  precipitates in this study corroborate so well with those in Seiler et al. (2023). Finally, a simpler mechanism may just involve adsorption of air  $\text{CO}_2$  to surface of powder crystals followed by desorption of a  $\text{CO}_2$  molecule of the original crystal lattice, followed by subsequent crystal lattice diffusion. In every case, gas-solid exchange equilibrium followed by significant  $^{14}\text{C}$  changes to  $\text{CaCO}_3$  original signal would require at least (a) the presence of very small crystals, and (b) longer duration of exposure to  $\text{CO}_2$ .

Even though we detected a difference in overall  $\text{CaCO}_3$  precipitate mass before and after heat treatments, our oxidative decomposition of carbonate by step-combustion (possibly more active on powder surfaces, than their interior) most likely removed just  $\text{H}_2\text{O}$  and interparticle adsorbed  $\text{CO}_2$ . Any other adsorbed  $\text{CO}_2$ , either deeply trapped in  $\text{CaCO}_3$  pores or bonded to the lattice, would contribute to the final  $^{14}\text{C}$  results we obtained.

We may never know for certain what is the mechanistic process of how ambient  $\text{CO}_2$  has altered Nydal's  $\text{CaCO}_3$  precipitates, and when this occurred during the 30+ years storage. Either way, several attempts to remove this exogenous carbon, e.g., after  $\text{HCl}$  and  $\text{H}_2\text{O}_2$  treatments, or chemically untreated flash-combustion (Seiler et al. 2023) as well as  $^{14}\text{C}$  two-step combustion oxidation method (this study) were insufficient to bring the 1963 and the 1980 series to expected  $^{14}\text{C}$  values.

As far as one can tell, all of Nydal's  $\text{CaCO}_3$  precipitates published in the literature yielded correct  $^{14}\text{C}$  values once measurements were completed and corrections were applied

(Nydal and Lövseth 1983, 1996). After 30+ years of storage, those same  $\text{CaCO}_3$  precipitates are yielding inaccurate  $^{14}\text{C}$  values. Neither Seiler et al. (2023) nor this study introduced artifacts to data to justify the differences detected. Hence, we can only assume that the current Nydal's  $\text{CaCO}_3$  precipitate archive is of no use to reproduce atmospheric  $^{14}\text{CO}_2$  signatures, until the contamination issue can be effectively resolved.

Carbon dioxide sequestration in the form of  $\text{CaCO}_3$  is a useful way to store atmospheric  $\text{CO}_2$  for further analyses. But it requires proper storage conditions, ideally within a hermetically sealed vial, such as evacuated flame-sealed glass ampoules.

#### **4. CONCLUSION**

Samples from the Lindesnes site (58°N), a small fraction of the large archive of atmospheric  $\text{CO}_2$  (as  $\text{CaCO}_3$ ) samples stored at NTNU since the 1960s, have been tested in this study. These samples have been previously  $^{14}\text{C}$  measured at NTNU after chemical cleansing procedures (e.g.,  $\text{HCl}$  and  $\text{H}_2\text{O}_2$ ) that attempted to remove surface contaminants.

Here, we applied a two-step oxidation treatment from room temperature to 285°C with air standard pressure. Our recent  $^{14}\text{C}$  results from a total of eight  $\text{CaCO}_3$  samples, associated with the atmospheric  $\text{CO}_2$  values of 1963 and 1980, did not differ significantly from those obtained by NTNU (Seiler et al. 2023). Like the NTNU values, they do not match with expected atmospheric  $^{14}\text{C}$  values. Our heating treatment worked well on reference materials of carbonate (FIRI-C) and organic (Rice char), mixed matrixes known to contain organic labile compounds, implying that the contaminant in  $\text{CaCO}_3$  samples is not OC and cannot be readily removed by low temperature heating. FTIR spectrum results indicate the presence of moisture. While their removal by heat did not improve  $^{14}\text{C}$  results per se, it gave insight to the current conditions of those  $\text{CaCO}_3$  samples.

To provide a new perspective on the elusive carbon contaminant of the Nydal's stored  $\text{CaCO}_3$  samples, we relied on notions of  $\text{CaCO}_3$  formation, growth and recrystallization. While numerous works have shown that  $\text{CO}_2$  to  $\text{CaCO}_3$  by  $\text{NaOH}$  reaction does, in principle, follow a straight pathway, calcium carbonate equilibria can be rather complex and influenced by several factors. However, in the case of  $\text{CaCO}_3$  precipitates that need to be stored for future  $^{14}\text{C}$  analysis, the use of a hermetically sealed vial for storage purposes would be the best practice.

#### **SUPPLEMENTARY MATERIAL**

To view supplementary material for this article, please visit <https://doi.org/10.1017/RDC.2023.106>

#### **ACKNOWLEDGMENTS**

We thank Jovany Merham, Evan Patrick Garcia, and Dr. Dima Fishman from the Laser Spectroscopy Labs, University of California, Irvine, for assistance on FTIR acquisition. We also wish to express our gratitude to the editors Tim Jull and Quan Hua, and 2 anonymous reviewers for their helpful comments and suggestions.

#### **CONFLICTS OF INTEREST**

The authors declare no conflict of interest.

## REFERENCES

- Beverly RK, Beaumont W, Tauz D, Ormsby KM, von Reden KF, Santos GM, Southon JR. 2010. The Keck carbon cycle AMS laboratory, University of California, Irvine: status report. *Radiocarbon* 52(2): 301–309.
- Bush SL, Santos GM, Xu X, Southon JR, Thiagarajan N, Hines SK, Adkins JF. 2013. Simple, rapid, and cost effective: a screening method for  $^{14}\text{C}$  analysis of small carbonate samples. *Radiocarbon* 55(2):631–640.
- Carol D. 1962. Rainwater as a chemical agent of geologic processes—a review. USGS water supply paper 1535-G:18.
- Currie LA, Benner BA, Cachier HA, Cary R, Chow JC, Urban DL, Eglinton TI, Gustafsson O, Hartmann PC, Hedges JI, Kessler JD. 2002. A critical evaluation of inter-laboratory data on total, elemental and isotopic carbon in the carbonaceous particle reference material. *Journal of Research of the National Institute of Standards and Technology* 107(3).
- Erans M, Nabavi SA, Manović V. 2020. Carbonation of lime-based materials under ambient conditions for direct air capture. *Journal of Cleaner Production* 242:118330.
- Febriada R, Cahyanto A, Herda E, Muthukanan V, Djustiana N, Faizal F, Panatarani C, Joni IM. 2021. Synthesis and characterization of porous  $\text{CaCO}_3$  vaterite particles by simple solution method. *Materials* 14(16):4425.
- Galwey AK, Brown ME. 1999. Studies in physical and theoretical chemistry. Chapter 12: Decomposition of carbonates. Volume 86:345–364. Elsevier. ISSN 0167-6881, ISBN 9780444824370, [https://doi.org/10.1016/S0167-6881\(99\)80014-7](https://doi.org/10.1016/S0167-6881(99)80014-7).
- Gao P, Xu X, Zhou L, Pack MA, Griffin S, Santos GM, Southon JR, Liu K. 2014. Rapid sample preparation of dissolved inorganic carbon in natural waters using a headspace-extraction approach for radiocarbon analysis by accelerator mass spectrometry. *Limnology and Oceanography: Methods* 12(4):174–190.
- Giacomin CE, Holm T, Mérida W. 2020.  $\text{CaCO}_3$  growth in conditions used for direct air capture. *Powder Technology* 370:39–47.
- Gupta U, Singh VK, Kumar V, Khajuria Y. 2015. Experimental and theoretical spectroscopic studies of calcium carbonate ( $\text{CaCO}_3$ ). *Materials Focus* 4(2):164–169.
- Hanein T, Simoni M, Woo CL, Provis JL, Kinoshita H. 2021. Decarbonisation of calcium carbonate at atmospheric temperatures and pressures, with simultaneous  $\text{CO}_2$  capture, through production of sodium carbonate. *Energy & Environmental Science* 14(12):6595–6604.
- Hinger EN, Santos GM, Druffel ER, Griffin S. 2010. Carbon isotope measurements of surface seawater from a time-series site off Southern California. *Radiocarbon* 52(1):69–89.
- Huang L, Zhang W, Santos GM, Rodríguez BT, Holden SR, Vetro V, Czimeczik CI. 2021. Application of the ECT9 protocol for radiocarbon-based source apportionment of carbonaceous aerosols. *Atmospheric Measurement Techniques* 14(5):3481–3500.
- Huang YC, Rao A, Huang SJ, Chang CY, Drechsler M, Knaus J, Chan JCC, Raiteri P, Gale JD, Gebauer D. 2021. Uncovering the role of bicarbonate in calcium carbonate formation at near-neutral pH. *Angewandte Chemie International Edition* 60(30):16707–16713.
- Levin I, Kromer B, Schoch-Fischer H, Bruns M, Münnich M, Berdau D, Vogel JC, Münnich KO. 1985. 25 years of tropospheric  $^{14}\text{C}$  observations in Central Europe. *Radiocarbon* 27(1):1–19.
- Liu X, Colman SM, Brown ET, Minor EC, Li H. 2013. Estimation of carbonate, total organic carbon, and biogenic silica content by FTIR and XRF techniques in lacustrine sediments. *Journal of Paleolimnology* 50(3):387–398.
- Maya JC, Chejne F, Gómez CA, Bhatia SK. 2018. Effect of the  $\text{CaO}$  sintering on the calcination rate of  $\text{CaCO}_3$  under atmospheres containing  $\text{CO}_2$ . *AIChE Journal* 64(10):3638–3648.
- Moore CH, Wade WJ. 2013. The nature and classification of carbonate porosity. In *Developments in sedimentology* (Vol. 67, pp. 51–65). Elsevier.
- NIST webbook. Available at: <https://webbook.nist.gov/>
- Nydal R, Lövsøth K. 1983. Tracing bomb  $^{14}\text{C}$  in the atmosphere 1962–1980. *Journal of Geophysical Research: Oceans* 88(C6):3621–3642.
- Nydal R, Lövsøth K. 1996. Carbon-14 measurements in atmospheric  $\text{CO}_2$  from northern and southern hemisphere sites, 1962–1993 (No. ORNL/CDIAC-93; NDP-057). Oak Ridge National Lab.(ORNL), Oak Ridge, TN (United States).
- Nydal R. 1966. Variation in the  $^{14}\text{C}$  concentration in the atmosphere during the last several years. *Tellus XVIII*:271–279.
- Reimer PJ, Brown TA, Reimer RW. 2004. Discussion: reporting and calibration of post-bomb  $^{14}\text{C}$  data. *Radiocarbon* 46(3):1299–1304.
- Sanz-Pérez ES, Murdock CR, Didas SA, Jones CW. 2016. Direct capture of  $\text{CO}_2$  from ambient air. *Chemical Reviews* 116(19):11840–11876.
- Santos GM, Alexandre A, Coe HH, Reyerson PE, Southon JR, De Carvalho CN. 2010. The phytolith  $^{14}\text{C}$  puzzle: a tale of background determinations and accuracy tests. *Radiocarbon* 52(1):113–128.
- Santos GM, Southon JR, Druffel-Rodríguez KC, Griffin S, Mazon M. 2004. Magnesium perchlorate as an alternative water trap in AMS graphite sample preparation: a report on sample preparation at KCCAMS at the University of California, Irvine. *Radiocarbon* 46(1):165–173.

- Santos GM, Southon JR, Griffin S, Beaupre SR, Druffel ERM. 2007. Ultra small-mass AMS  $^{14}\text{C}$  sample preparation and analyses at KCCAMS/UCI Facility. *Nuclear Instruments and Methods in Physics Research Section B: Beam Interactions with Materials and Atoms* 259(1): 293–302.
- Santos GM, Xu X. 2017. Bag of tricks: a set of techniques and other resources to help  $^{14}\text{C}$  laboratory setup, sample processing, and beyond. *Radiocarbon* 59(3):785–801. <https://doi.org/10.1017/RDC.2016.43>
- Sanz-Pérez ES, Murdock CR, Didas SA, Jones CW. 2016. Direct capture of  $\text{CO}_2$  from ambient air. *Chemical Reviews* 116(19):11840–11876.
- Scott EM, Boaretto E, Bryant C, Cook GT, Gulliksen S, Harkness DD, Heinemeier J, McGee E, Naysmith P, Possnert G, van der Plicht H. 2004. Future needs and requirements for AMS  $^{14}\text{C}$  standards and reference materials. *Nuclear Instruments and Methods in Physics Research Section B: Beam Interactions with Materials and Atoms* 223:382–387.
- Seiler M, Grootes PM, Svarva H, Nadeau MJ. 2023. The Radiocarbon Sample Archive of Trondheim. *Radiocarbon*. DOI:10.1017/RDC.2023.57
- Stern KH. 1969. High Temperature properties and decomposition of inorganic salts, Part 2. Carbonates. Commerce Department, National Institute of Standards and Technology (NIST). NBS National Standard Reference Data Series (NSRDS) 30:C 13.48
- Stuiver M, Polach HA. 1977. Discussion reporting of  $^{14}\text{C}$  data. *Radiocarbon* 19(3):355–363.
- Szidat S, Bench G, Bernardoni V, Calzolari G, Czimeczik CI, Derendorp L, Dusek U, Elder K, Fedi ME, Genberg J. et al. 2013. Intercomparison of  $^{14}\text{C}$  analysis of carbonaceous aerosols: exercise 2009. *Radiocarbon* 55(3):1496–1509.
- Vorres KS. 1990. The Argonne premium coal sample program. *Energy & Fuels* 4(5):420–426.
- Toffolo MB. 2020. Radiocarbon dating of anthropogenic carbonates: what is the benchmark for sample selection? *Heritage* 3(4):1416–1432.
- Turnbull JC, Mikaloff Fletcher SE, Brailsford GW, Moss RC, Norris MW, Steinkamp K. 2017. Sixty years of radiocarbon dioxide measurements at Wellington, New Zealand: 1954–2014. *Atmospheric Chemistry and Physics* 17(23):14771–14784.
- Yoon H, Major J, Dewers T, Eichhubl P. 2017. Application of a pore-scale reactive transport model to a natural analog for reaction-induced pore alterations. *Journal of Petroleum Science and Engineering*, 155:11–20.
- Zeman FS, Lackner KS. 2004. Capturing carbon dioxide directly from the atmosphere. *World Resource Review* 16(2):157–172.